ARTICLES

nature medicine

Inhibition of hypothalamic carnitine palmitoyltransferase-1 decreases food intake and glucose production

Silvana Obici[1], Zhaohui Feng[1], Arduino Arduini[2,3], Roberto Conti[2] & Luciano Rossetti[1]

The enzyme carnitine palmitoyltransferase-1 (CPT1) regulates long-chain fatty acid (LCFA) entry into mitochondria, where the LCFAs undergo β-oxidation. To investigate the mechanism(s) by which central metabolism of lipids can modulate energy balance, we selectively reduced lipid oxidation in the hypothalamus. We decreased the activity of CPT1 by administering to rats a ribozyme-containing plasmid designed specifically to decrease the expression of this enzyme or by infusing pharmacological inhibitors of its activity into the third cerebral ventricle. Either genetic or biochemical inhibition of hypothalamic CPT1 activity was sufficient to substantially diminish food intake and endogenous glucose production. These results indicated that changes in the rate of lipid oxidation in selective hypothalamic neurons signaled nutrient availability to the hypothalamus, which in turn modulated the exogenous and endogenous inputs of nutrients into the circulation.

Complex metabolic diseases such as obesity and type 2 diabetes mellitus are the result of multiple interactions between genes and environment[1,2]. Hypothalamic centers sense the availability of peripheral nutrients partly through redundant nutrient-induced peripheral signals such as leptin and insulin[3–9] as well as through direct metabolic signaling[10–13]. Lipid metabolism in selective hypothalamic neurons may be a primary biochemical sensor for nutrient availability, which in turn exerts a negative feedback on food intake[10–13] and endogenous glucose production[11]. Here we explore the mechanism responsible for the lipid-dependent signal by examining the function of hypothalamic lipid oxidation. The enzyme CPT1 regulates the entry of LCFAs into mitochondria, where they undergo β-oxidation[14,15]. Two observations drove our attention to the possible involvement of hypothalamic CPT1 (**Fig. 1a**). First, the suppressive effect of inhibitors of fatty acid synthase on food intake requires increased malonyl coenzyme A (malonyl-CoA), a potent inhibitor of CPT1 activity[10]. Second, the suppressive effects of the LCFA oleic acid, delivered into the third cerebral ventricle (intracerebroventricular (ICV) administration), on food intake and on glucose production are not replicated by equimolar administration of octanoic acid, a medium-chain fatty acid that does not require CPT1 for entry into mitochondria[11]. Based on those findings, we postulated that an increase in neuronal LCFA-CoA would be a hypothalamic signal of nutrient availability. This increase could be generated by either the ICV administration of LCFA molecules (such as oleic acid)[11] or the inhibition of the entry of LCFA-CoA molecules into mitochondria because of increased malonyl-CoA[10]. To test this, we sought to determine whether a primary decrease in CPT1 activity in the hypothalamus was sufficient to inhibit both feeding behavior and glucose production.

RESULTS

Molecular and pharmacological approaches to CPT1 inhibition

To inhibit the entry of LCFA-CoA molecules into mitochondria, we used pharmacological and molecular approaches. We first showed by northern blot analysis that the prevalent form of CPT1 in the hypothalamus was the liver (CPT1L) rather than the muscle (CPT1M) isoform (**Fig. 1b**). We therefore designed a ribozyme (CPT1L-Ribo; **Fig. 1c**) that specifically cleaved *CPT1A* (liver isoform) mRNA, and introduced it into a mammalian expression vector (**Fig. 1d**). We then tested the ability of this construct to decrease CPT1L expression in stably transfected AtT20 cells (**Fig. 1e,f**). We also showed that systemic infusion of CPT1 inhibitors substantially increased the concentration of LCFA-CoA molecules in liver and skeletal muscle (**Fig. 1g**). Thus, we validated the use of CPT1L-Ribo to decrease CPT1 expression in mammalian cells and provided evidence that inhibition of CPT1 activity was itself sufficient to increase the tissue concentration of LCFA-CoA.

Based on those results, we administered either one of two specific CPT1 inhibitors (the reversible CPT1L inhibitor (*R*)-*N*-(tetradecylcarbamoyl)-aminocarnitine (ST1326) or 2-tetradecylglydate (TDGA), or CPT1L-Ribo by ICV infusion into conscious rats to decrease CPT1 activity and increase the amount of LCFA-CoA in the hypothalamus. The baseline anthropometrical and biochemical characteristics of rats in each experimental group were similar to those of the appropriate control (**Table 1**). There was a tendency toward lower fasting plasma insulin and leptin in rats treated by ICV infusion of CPT1L-Ribo for 3 d than in control rats whose food intake was matched (pair feeding) to that of the rats treated with CPTL-Ribo (**Table 1**).

We implanted ICV catheters into male Sprague-Dawley rats by stereotactic surgery[11,16,17]. We did the biochemical and molecular

[1]Departments of Medicine and Molecular Pharmacology, Diabetes Research and Training Center, Albert Einstein College of Medicine, 1300 Morris Park Avenue, Bronx, New York 10461, USA. [2]Department of Metabolism & Endocrinology, Sigma Tau Pharmaceutical Industries, Via Pontina km 30,400, 00040 Pomezia, Italy. [3]Present address: F. Hoffmann-La Roche Ltd., Pharmaceutical Division, Vascular & Metabolic Diseases, CH-4070 Basel, Switzerland. Correspondence should be addressed to L.R. (rossetti@aecom.yu.edu).

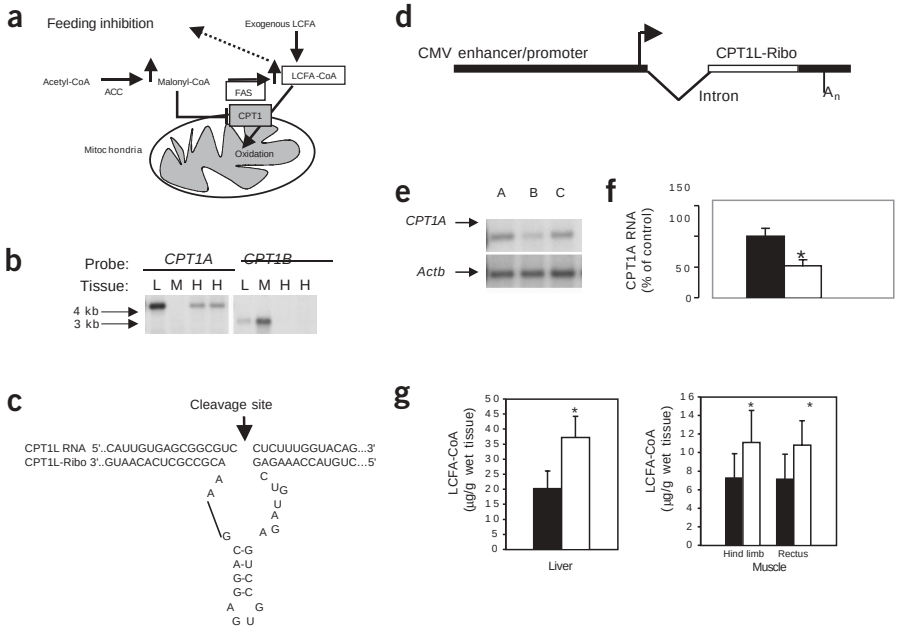

Figure 1 Inhibition of hypothalamic CPT1. (**a**) Proposed model for function of CPT1 in hypothalamic regulation of food intake. Anorectic drugs such as fatty acid synthase (FAS) inhibitors increase malonyl-CoA, which is derived from the carboxylation of acetyl-CoA by the enzyme acetyl-CoA carboxylase (ACC). Large amounts of malonyl-CoA inhibit CPT1-dependent oxidation of LCFA-CoA molecules. ICV administration of exogenous fatty acids (LCFAs) directly increases cellular LCFA-CoA. The resulting increase in intracellular LCFA-CoA concentration leads to inhibition of feeding behavior. (**b**) Northern blot analysis of CPT1 expression in whole rat hypothalamus. Left, a probe specific for *CPT1A* showed a band of about 4.3 kb (arrow, left margin) in the liver (L) and in hypothalamus (H), but not in hind limb muscle (M). Right, hybridization with a *CPT1B*-specific probe showed a band of ~3 kb (arrow, left margin) in liver (L) and muscle (M), but not in hypothalamus (H). (**c**) Design of a ribozyme selective for *CPT1A* mRNA. The CPT1L-Ribo transcript (lower sequence) contained a central sequence with a stem-loop structure typical of a hammerhead ribozyme, flanked by sequences that hybridized to the target *CPT1A* mRNA (upper sequence). Arrow, predicted cleavage site. (**d**) Construction of a CPT1L-Ribo plasmid. The CPT1L-Ribo fragment was cloned into a mammalian expression vector (pTarget) under control of a CMV promoter and immediately downstream of an intron cassette and upstream of a simian virus 40 polyadenylation signal (A_n). Arrow indicates initiation of transcription of the ribozyme. (**e**) Northern blot of AtT20 cells transfected with vector alone (lane A) or CPT1L-Ribo plasmid (lane B), or not transfected (lane C). Blots were hybridized with *CPT1A* probe (top) or β-actin (*Actb*; bottom). (**f**) Quantification of AtT20 northern blots. Cells expressing CPT1L-Ribo (□) contained ~50% less *CPT1A* mRNA than control cells transfected with vector alone (■). Data were expressed as percent of control after normalization with β-actin expression. (**g**) Systemic administration of CPT1 inhibitors increased intracellular LCFA-CoA, measured by HPLC in liver and skeletal muscle tissues of rats infused intravenously with vehicle (■) or CPT1 inhibitors (□). *, $P < 0.01$.

analyses and the metabolic and feeding experiments about 3 weeks later, after rats had completely recovered from the operation (**Fig. 2a**). CPT1L-Ribo was delivered by ICV injection 3 d before experimental tests (**Fig. 2a**). CPT1 inhibitors or vehicle were acutely injected or administered by ICV infusion for 6 h in continuously catheterized Sprague Dawley rats[11,16] (**Fig. 2a**). We first examined the effect of CPT1L-Ribo on *CPT1A* (liver isoform; **Fig. 2b**) and *CPT1B* (muscle isoform; **Fig. 2c**) mRNA in selected hypothalamic nuclei from which we obtained samples using a 'micropunch' procedure. Using quantitative real-time PCR (adjusted for β-actin copy number), we first confirmed the accuracy of our arcuate nuclei (ARC) sampling by comparing the abundance of selected transcripts (pro-opiomelanocortin and agouti-related protein) in 'micropunches' of ARC and of immediately lateral areas. The mRNA of these markers was present in large amounts only in the ARC 'micropunches' (data not shown). We next showed a substantial decrease in *CPT1A* mRNA in ARC, but not in other regions of the hypothalamus, such as the paraventricular nuclei or the lateral hypothalamus. Conversely, much less *CPT1B* mRNA was expressed, particularly in ARC, and its expression was not appreciably altered by CPT1L-Ribo.

If the considerable decrease in *CPT1A* mRNA had important biological effects, it should also have led to a decrease in CPT1 activity in ARC. Thus, we next measured CPT1 activity in ARC and in whole hypothalamus. We found a considerable decrease in CPT1 activity (**Fig. 2d**) after ICV administration of CPT1L-Ribo in ARC but not in whole hypothalamus (**Fig. 2e**), in accord with the selective effects found on *CPT1A* mRNA (**Fig. 2b**). We also confirmed the effect of the irreversible CPT1 inhibitor TDGA on CPT1 activity in ARC (**Fig. 2d**) and whole hypothalamus (**Fig. 2e**). Finally, we tested whether ICV administration of inhibitors of CPT1L activity led to increased LCFA-CoA in ARC. We administered the reversible CPTL1 inhibitor ST1326 (25 pmol delivered as a bolus) or its inactive stereoisomer (*S*)-*N*-(tetradecylcarbamoyl)-aminocarnitine (ST1340; control) by ICV injection, and measured individual types of LCFA-CoA in isolated hypothalamic nuclei after 48 h. ICV administration of ST1326 led to a substantial increase in stearoyl-CoA (**Fig. 2f**) and oleyl-CoA (**Fig. 2g**) in ARC but not in paraventricular nuclei and lateral hypothalamus. Other types of LCFA-CoA (data not shown) were also substantially increased by ICV administration of ST1326. Thus, ICV delivery of a molecular and pharmacological inhibitor of CPT1 effectively decreased CPT1 activity in ARC, and the inhibition of CPT1L activity substantially increased the concentrations of specific types of LCFA-CoA.

Hypothalamic inhibition of CPT1 decreased food intake

Based on the findings described above, we designed two sets of experiments to examine the effects of the hypothalamic inhibition of CPT1 activity on feeding behavior and insulin action. First, we examined whether central administration of molecular and pharmacological antagonists of CPT1 modulated feeding behavior in conscious rats (**Fig. 3**). At 3 h before the onset of the dark cycle, paired groups of rats received a bolus of either control vector or CPT1L-Ribo, or ST1340 or ST1326, through an indwelling ICV catheter. We monitored food intake in 'metabolic' cages before and up to 72 h after the ICV injections[11]. The selective decrease in ARC CPT1L expression and activity (**Fig. 2b,d**) through ICV injection of CPT1L-Ribo resulted in rapid onset of anorexia (**Fig. 3a–c**) starting on the first night after the ICV administration (average food intake, 13.0 ± 1.9 g/d versus 23.0 ± 3.2 g/d (CPTL-Ribo group

versus control vector on day 1); $P < 0.01$). The effect of ICV administration of CPT1L-Ribo on food intake was significant compared with that of control vector or an unrelated control ribozyme (**Fig. 3c**). Similarly, acute ICV injection of a potent and specific inhibitor of CPT1L (ST1326) substantially inhibited food intake in rats, whereas its inactive stereoisomer (ST1340) failed to modify feeding behavior (**Fig. 3d,e**). The anorectic effect of central CPT1 inhibition lasted for at least 48 h after a single ICV administration. These decreases in food intake were significant ($P < 0.001$ compared with both baseline and vehicle or control (**Fig. 3a–e**). The changes from baseline induced by CPT1 inhibition were statistically significant at 24 h (–17.6 ± 2.0 g and –12.4 ± 3.9 g) and 48 h (–13.4 ± 1.8 g and –7.8 ± 3.8 g) after ICV administration of CP1L-Ribo and a large dose of ST1326, respectively (**Fig. 3b,e**). This represented a decrease in daily food intake of about 50%, which returned toward baseline values by 72 h.

Table 1 Characteristics of the experimental groups before and during the pancreatic-insulin clamp studies

	Vector	CPT1L-Ribo	Vehicle	TDGA	ST1340	ST1326
Basal:						
Body weight (g)	286 ± 9	277 ± 8	345 ± 13	319 ± 10	307 ± 6	302 ± 4
Food intake (g)	13 ± 3	14 ± 2	25 ± 2	25 ± 2	22 ± 3	21 ± 2
Glucose (mM)	8.1 ± 0.7	8.2 ± 0.6	8.1 ± 0.5	8.2 ± 0.8	8.0 ± 1.0	8.1 ± 0.7
Insulin (ng/ml)	1.2 ± 0.2	0.8 ± 0.2	2 ± 0.4	1.9 ± 0.1	1.4 ± 0.2	1.4 ± 0.2
FFA (mM)	0.6 ± 0.1	0.5 ± 0.1	0.6 ± 0.1	0.5 ± 0.1	0.4 ± 0.1	0.5 ± 0.1
Leptin (ng/ml)	1.0 ± 0.3	0.8 ± 0.1	1.5 ± 0.2	1.7 ± 0.1	0.9 ± 0.2	0.9 ± 0.1
Clamp:						
Glucose (mM)	8.0 ± 0.8	8.1 ± 0.5	8.0 ± 0.8	8.1 ± 0.5	8.2 ± 0.9	8.1 ± 0.8
Insulin (μU/ml)	20 ± 2	21 ± 2	21 ± 2	25 ± 3	25 ± 4	21 ± 2
FFA (mM)	0.4 ± 0.1	0.4 ± 0.1	0.6 ± 0.1	0.5 ± 0.1	0.4 ± 0.1	0.4 ± 0.1

The values during the clamp represent steady-state levels obtained by averaging the results of at least four plasma samples during the experimental period. Food intake in the vector group was matched to that of the CPT1L-Ribo group. Food intake in the other groups was measured before the acute ICV infusion of test substances. FFA, free fatty acids.

To begin investigating the mechanisms responsible for the anorectic properties of ARC CPT1 inhibition, we next analyzed the effect of CPT1L-Ribo on the gene expression of key ARC peptides. Quantitative analyses by real-time PCR showed a considerable decrease in agouti-related protein and neuropeptide Y mRNA in the ARC of rats treated with ICV administration of CPT1L-Ribo compared with that of rats given the unrelated control ribozyme (**Fig. 3f**). Conversely, the expression of pro-opiomelanocortin in the ARC was not altered by CPT1L-Ribo administration (**Fig. 3f**).

Overall, these anorectic effects support the idea that changes in neuronal concentrations of LCFA-CoA molecules may directly control food intake through their action on discrete hypothalamic centers. Furthermore, increases in LCFA-CoA in selective hypothalamic neurons were likely to account for the potent effects of oleic acid and fatty acid synthase inhibitors on food intake[10–13].

Hypothalamic inhibition of CPT1 inhibited glucose production

We also designed experiments to examine the effect of central inhibition of CPT1 on whole-body insulin action (**Fig. 4a,b**). We assessed insulin action by a combination of ICV infusions with systemic pancreatic-insulin clamp studies (**Fig. 4b**). The daily food intake was matched in the rats receiving ICV administration of vector or CPT1L-Ribo (**Table 1**). All rats also received an intra-arterial infusion of [^{3}H]glucose for the last 4 h of ICV infusion and a pancreatic-insulin clamp (insulin, 1 mU/kg per min; somatostatin, 3 μg/kg per min) during the last 2 h of the study[11,16]. As expected, in the presence of approximately basal amounts of circulating insulin (clamp procedure; **Table 1**), the rate of glucose infusion required to maintain euglycemia was marginal in ICV control studies (rats infused with vector-ST1340 or vehicle; ~0.8 mg/kg per min). In contrast, after ICV infusion of inhibitors of CPT1 expression or activity, glucose had to be infused at a rate of ~5 mg/kg per min to prevent hypoglycemia. Thus, central inhibition of CPT1 activity in the presence of fixed and basal insulin

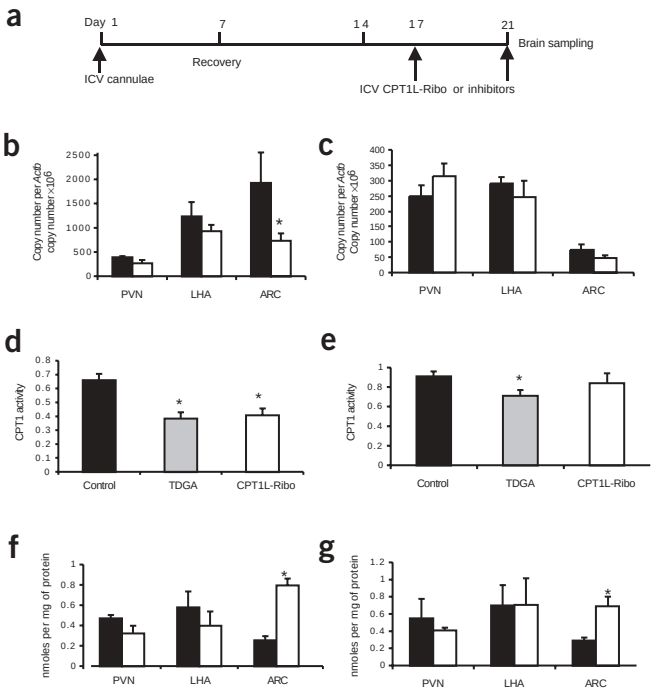

Figure 2 Genetic or pharmacological inhibition of CPT1 in ARC reduced CPT1 activity and increased LCFA-CoA. (**a**) ICV cannulae were surgically implanted on day 1 (~3 weeks before the *in vivo* study). Full recovery of body weight and food intake was achieved by day 7. Rats were given an ICV injection of CPT1L-Ribo or controls on day 17. The experimental group treated with TDGA received ICV injection of the inhibitor on day 21, 6 h before brains were collected. (**b,c**) Quantification of *CPT1A* (**b**) and *CPT1B* (**c**) Quantification of mRNA by real-time PCR. ■, ICV injection of pTarget control ($n = 4$); □, CPT1L-Ribo ($n = 5$). The copy number of *CPT1* mRNA was normalized to the *Actb* copy number × 10^6. (**d,e**) CPT1 activity in individual ARC (**d**) or whole hypothalamus (**e**). ■, ICV control injections ($n = 6$; received aCSF + 2% DMSO or control ribozyme); ■, TDGA ($n = 6$) □, CPTL-Ribo ($n = 5$). (**f,g**) ICV administration of CPT1 inhibitors increased LCFA-CoA in ARC. Stearoyl-CoA (**f**) and oleyl-CoA (**g**) were measured by HPLC in ARC of rats after ICV injection of ST1340 (■) or ST1326 (□), respectively. PVN, paraventricular nuclei; LHA, lateral hypothalamus. *, $P < 0.001$.

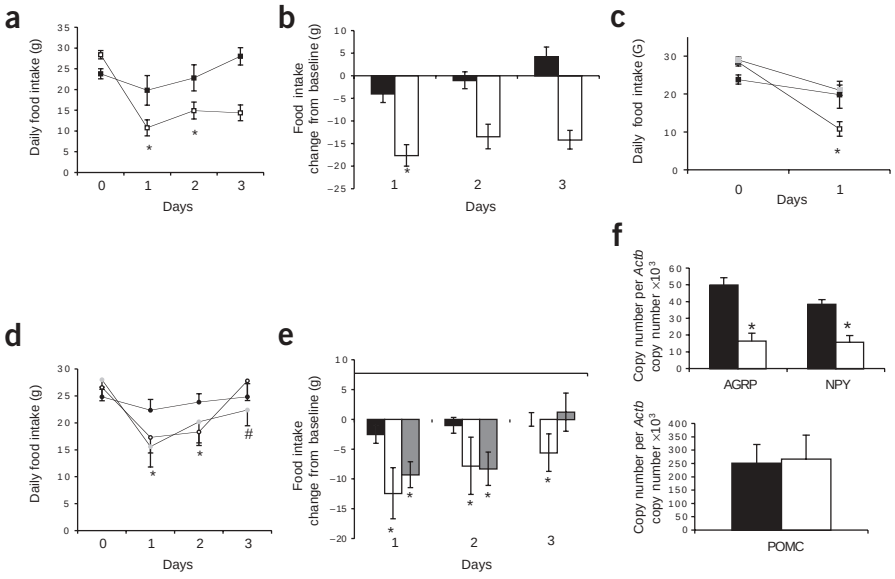

Figure 3 Inhibition of hypothalamic CPT1L by genetic or pharmacological means decreased food intake. (**a**) On day 0, rats received a single ICV injection of CPT1L-Ribo (□) or control vector (■). (**b**) Changes in food intake induced by ICV administration of CPT1L-Ribo (□) or vector injection (■). (**c**) Effect on 24-h food intake by ICV injection of CPT1L-Ribo (□) compared with ICV injection of vector control (■) or ribozyme control (■). (**d**) Daily food intake after a single ICV injection on day 0 of either ST1326 (5 pmol, ○; 25 pmol, ●), or of the inactive stereo isomer ST1340 (25 pmol, ●). (**e**) Changes in food intake induced by ICV administration of ST1326 (5 pmol, ■ and 25 pmol, □, respectively) or control ST1340 (■). *, $P < 0.001$ versus control group and baseline; #, $P < 0.01$ only for high-dose ST1326 versus control. (**f**) Downregulation of CPT1L by ICV administration of CPT1L-Ribo decreased expression of neuropeptide Y and agouti-related protein in ARC. Quantitative analysis by real-time PCR of neuropeptide Y (NPY) and agouti-related protein (AGRP; both top) and pro-opiomelanocortin (POMC; bottom) in ARC of rats treated with vector control (■) or CPT1L-Ribo (□). *, $P < 0.001$; #, $P < 0.01$.

concentrations stimulated insulin action on glucose homeostasis.

We next examined the potential mechanism(s) by which ICV administration of CPT1 antagonists enhanced whole-body insulin action. We assessed glucose kinetics by tracer dilution methodology[11,16] to establish whether the increased rate of glucose infusion induced by central antagonists of CPT1 was because of stimulation of glucose uptake or suppression of endogenous glucose production. The rate of glucose uptake was not significantly affected by ICV treatments (**Fig. 4c,e,g**). Conversely, in the presence of basal and equal amounts of insulin (~20 μU/ml), glucose production was substantially and significantly decreased (**Fig. 4d,f,h**) by ICV administration of CPT1L-Ribo (by 30 ± 3%; $n = 5$), ST1326 (by 44 ± 7%; $n = 8$) or TDGA (by 47 ± 6%; $n = 7$). These decreases in glucose output completely accounted for the effect of central inhibition of CPT1 on whole-body glucose metabolism.

DISCUSSION

On the basis of our results, we concluded that the central inhibition of CPT1 activity was sufficient to substantially suppress food intake and endogenous glucose production. Furthermore, we propose that the central inhibition of CPT1 activity led to increased LCFA-CoA in selective hypothalamic neurons. This increase represented a central signal of 'nutrient abundance', which in turn activated a chain of neuronal events designed to promote a switch in fuel sources from carbohydrates to lipids and to limit the further entry of exogenous and endogenous nutrients into the circulation.

Along with the demonstration of the potent effects of the central delivery of the LCFA oleic acid and of fatty acid synthase inhibitors[10–13], our findings supported the idea that an increase in cellular LCFA-CoA in hypothalamic neurons was an important sensor of increased nutrient availability (**Fig. 1a**). This in turn activated central neuronal pathways involved in the regulation of both energy homeostasis and hepatic insulin action. As glucose production by the liver is the main source of endogenous fuel, central neural circuitries concomitantly modulate exogenous and endogenous sources of energy[11,16]. This is consistent with a negative feedback system designed to monitor and regulate the input of nutrients in the circulation in response to changes in their availability.

As circulating free fatty acids can gain access to the central nervous system[18–19], changes in hypothalamic fatty acid oxidation are likely to modulate the regulation of energy balance and insulin action through changes in neuronal amounts of LCFA-CoA. In physiological conditions, inhibition of hypothalamic CPT1 activity is likely to occur when neuronal malonyl-CoA is increased. An increase in cellular malonyl-CoA is generally induced by increased metabolism of carbohydrates. Thus, this hypothetical 'central lipid signal' would be generated when availability of LCFAs is coupled with increased availability of carbohydrates (increased malonyl-CoA). As inhibition of hypothalamic CPT1 activity itself reproduced the effects of ICV administration of the LCFA oleic acid[11] on food intake and glucose production, it is likely that the accumulation of LCFA-CoA molecules rather than their flux into the mitochondria is a key component of hypothalamic lipid sensing. This is also consistent with the observation that a considerable increase in the availability of the medium-chain fatty acid octanoic acid[11] did not reproduce the potent effects of oleic acid on glucose production[11]. Although our report has provided evidence for the importance of esters of LCFAs in hypothalamic lipid sensing, it is still possible that direct interactions of medium- and long-chain fatty acids with cellular receptors may mediate some of their biological effects[20]. Moreover, although malonyl-CoA is likely to be important in the physiological regulation of hypothalamic CPT1 activity, it is unlikely that an increase in malonyl-CoA occurred here in the presence of genetic or pharmacological inhibition of CPT1 activity. In fact, inhibition of CPT1 activity results in increased amounts of LCFA-CoA, which in turn decreases malonyl-CoA through inhibition of acetyl-CoA carboxylase[21,22].

Finally, the potent orexigenic (appetite-stimulating) effects of cannabinoids and the potent anorectic effects of CB_1 receptor[23] antagonism may also be partly mediated through modulation of hypothalamic CPT1 activity and of LCFA-CoA. In fact, endocannabinoids stimulate CPT1 activity and fatty acid oxidation in cultured astrocytes independently of malonyl-CoA and through interaction with CB_1 receptors[24]. Finally, central inhibition of fatty acid oxidation may represent an innovative approach to the prevention and treatment of obesity and type 2 diabetes mellitus.

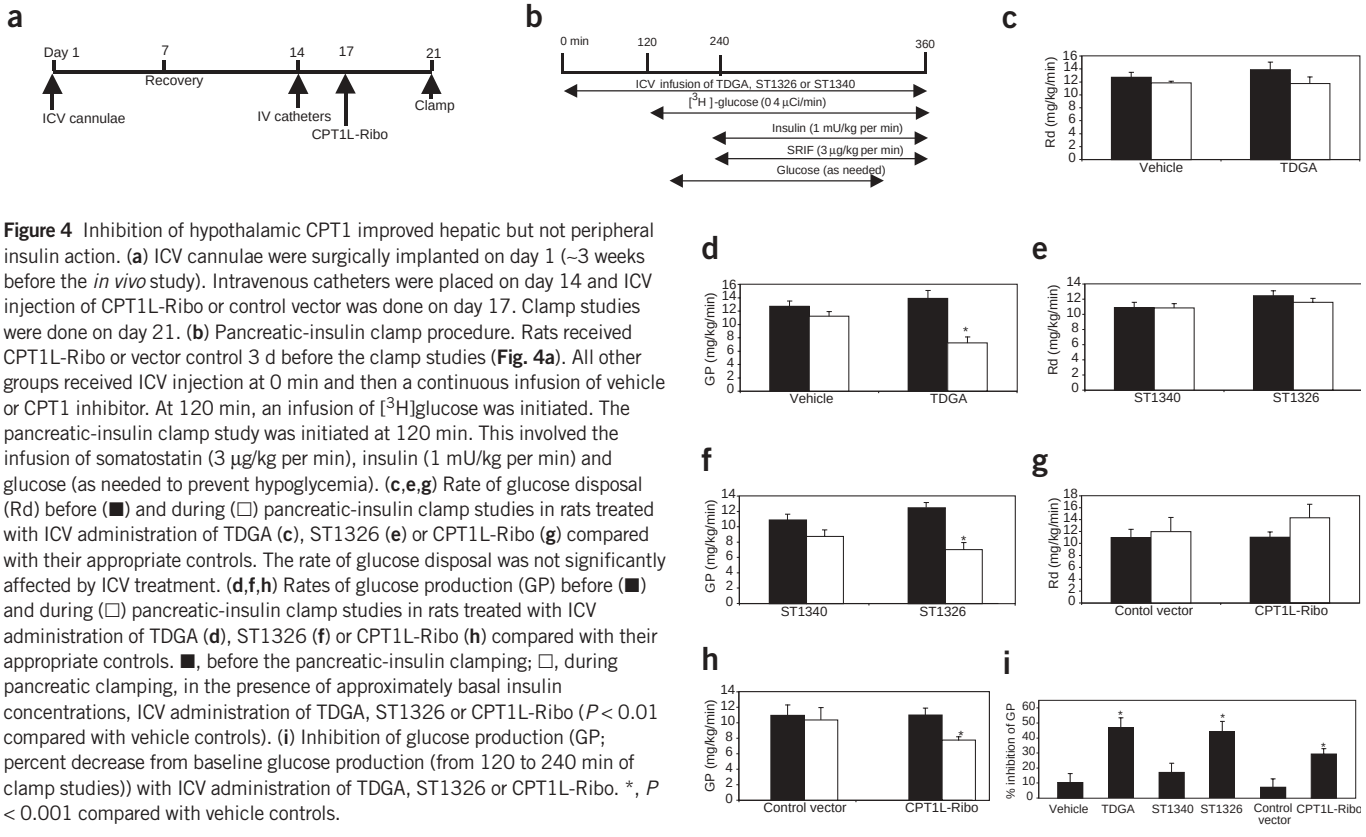

Figure 4 Inhibition of hypothalamic CPT1 improved hepatic but not peripheral insulin action. (**a**) ICV cannulae were surgically implanted on day 1 (~3 weeks before the *in vivo* study). Intravenous catheters were placed on day 14 and ICV injection of CPT1L-Ribo or control vector was done on day 17. Clamp studies were done on day 21. (**b**) Pancreatic-insulin clamp procedure. Rats received CPT1L-Ribo or vector control 3 d before the clamp studies (**Fig. 4a**). All other groups received ICV injection at 0 min and then a continuous infusion of vehicle or CPT1 inhibitor. At 120 min, an infusion of [^{3}H]glucose was initiated. The pancreatic-insulin clamp study was initiated at 120 min. This involved the infusion of somatostatin (3 μg/kg per min), insulin (1 mU/kg per min) and glucose (as needed to prevent hypoglycemia). (**c**,**e**,**g**) Rate of glucose disposal (Rd) before (■) and during (□) pancreatic-insulin clamp studies in rats treated with ICV administration of TDGA (**c**), ST1326 (**e**) or CPT1L-Ribo (**g**) compared with their appropriate controls. The rate of glucose disposal was not significantly affected by ICV treatment. (**d**,**f**,**h**) Rates of glucose production (GP) before (■) and during (□) pancreatic-insulin clamp studies in rats treated with ICV administration of TDGA (**d**), ST1326 (**f**) or CPT1L-Ribo (**h**) compared with their appropriate controls. ■, before the pancreatic-insulin clamping; □, during pancreatic clamping, in the presence of approximately basal insulin concentrations, ICV administration of TDGA, ST1326 or CPT1L-Ribo ($P < 0.01$ compared with vehicle controls). (**i**) Inhibition of glucose production (GP; percent decrease from baseline glucose production (from 120 to 240 min of clamp studies)) with ICV administration of TDGA, ST1326 or CPT1L-Ribo. *, $P < 0.001$ compared with vehicle controls.

METHODS

Design and cloning of CPT1L-Ribo. Two complementary oligonucleotides (ODN) 51 base pairs in length (5′-CTGTACCAAAGAGCTGATGAGTCCGTGAGGACGAAACGCCGCTCACAATGA-3′, and 5′-CATTGTGAGCGGCGTTTCGTCCTCACGGACTCATCAGCTCTTTGGTACAGA-3′) were synthesized (Operon Technologies). These contained the catalytic core of a hammerhead ribozyme sequence (underlined; **Fig. 1c**), flanked by a 13-nucleotide-long sequence from *CPT1A*[25,26]. After annealing, the double-stranded ODN was inserted into a mammalian expression vector, pTarget (Stratagene; **Fig. 1d**). Control studies used either pTarget vector alone, where indicated, or a ribozyme control plasmid (RiboC) in which the CPT-specific sequences were replaced by an unrelated sequence (underlined; 5′-GGAGCCTCGAGATCTGATGAGTCCGTGAGGACGAAACTGTGAGCGTTTGG-3′).

Expression of CPT1L ribozyme. CPT1L-Ribo plasmid or vector alone was transfected into AtT20 cells with polyethylenimine (Sigma-Aldrich)[27]. Northern blot analysis was done on a pool of ~200 independent clones. For *in vivo* expression, a complex of CPT1lL-Ribo plasmid and polyethylenimine was made and given by ICV injection as described before[28].

Brain stereotactic 'micropunches'. Brain 'micropunches' of individual hypothalamic nuclei were prepared as described before[29–31]. Rat brains were rapidly removed and frozen in isopentane on dry ice at a temperature of 15 °C for 5 min. The brain was then implanted frozen on a pedestal and placed in the cryostat and maintained at a temperature of –15 °C. Brain sections 500 μm in thickness were made and mounted onto glass slides. Using anatomical landmarks from a rat brain stereotactic atlas[31], individual nuclei were punched out using a stainless steel needle. The accuracy and reproducibility of the punches was established by inspecting the topography of the holes by trans-illumination under a low-power light microscope and by measuring the expression of selected transcripts[30].

Quantitation of *CPT1* and neuropeptide mRNA by northern blot analysis and real-time PCR. CPT1L probes spanned 755 nucleotides from position 10 to position 765 of *CPT1A* cDNA (GenBank accession number, L07736); the CPT1M probe spanned 545 nucleotides from position 688 to position 1,233 of *CPT1B* cDNA (GenBank accession number, NM_013200).

Total RNA was isolated with Trizol (Invitrogen) from individual hypothalamic nuclei. Single-stranded cDNA synthesis and real-time PCR reactions were done as described before[30]. *CPT1A* and *CPT1B* mRNA primers contained the following sequences:CPT1L,forward,5′-CTCCGAGCTCAG TGAGGACCTAAAG-3′ and reverse, 5′-CAAATACCACTGCAATTTGTG-3′; and CPT1M, forward, 5′-CCAGACTGCAGAAATACCTGGTGCTC-3′ and reverse, 5′-GTTCTGACGTGCTTCTGCCCACTCTAC-3′. Hypothalamic neuropeptide expression was measured by real-time PCR using the following primers: neuropeptide Y, forward, 5′-GCCATGATGCTAGGTAACAAACG-3′ and reverse, 5′-GTTTCATTTCCCATCACCACATG-3′; pro-opiomelanocortin, forward, 5′-CCAGGCAACGGAGATGAAC-3′ and reverse, 5′-TCACTGGCC CTTCTTGTGC-3′; agouti-related protein, forward, 5′-GCCATGCTGACTGCAATGTT-3′ and reverse, 5′-TGGCTAGGTGCGACTACAGA-3′; and β-actin, forward, 5′-TGAGACCTTCAACACC CCAGCC-3′ and reverse,5′-GAGTACTTGCGCTCAGGAGGAG-3′. The copy number of each transcript was measured against a copy-number standard curve of cloned target templates. Expression of each transcript was normalized to the copy number for β-actin. Normalization with the glyceraldehyde phosphodehydrogenase copy number yielded similar results (data not shown).

Animal preparation for the *in vivo* experiments. We studied 10-week-old male Sprague-Dawley rats (Charles River Breeding Laboratories). Indwelling catheters were placed in the third cerebral ventricle[11,16,17] and in the internal jugular vein and carotid artery[16,17].

Effect of central inhibition of CPT1 and food intake. We measured the effects of ICV administration of CPT1L-Ribo and ST1326 on food intake.

Daily food intake was constant (changes, <10%) for a minimum of three consecutive days preceding the ICV injections. At 3 h before the start of the dark cycle, CPT1L-Ribo, vector control, ST1326 or ST1340 was administered by ICV injection. Rats received single bolus injections of ST1340 (25 pmol) or ST1326 (5 or 25 pmol). Food intake was monitored for the ensuing 72 h.

Assay for CPT activity. ARC obtained by the 'micropunch' technique were homogenized in 70 µl buffer containing 0.25 M sucrose, 1 mM EDTA and 10 mM Tris-HCl, pH 7.4. The homogenate was fractionated by centrifugation at 20,000*g* for 20 min. CPT enzymatic activity was measured in the post-microsomal fraction as described before[32].

Measurement of long-chain acyl-CoA esters. Long-chain acyl-CoA esters were extracted from a pool of hypothalamic nuclei obtained from five rats treated with ICV administration of ST1340 or ST1326. LCFA-CoA was extracted and measured as described before[33].

***In vivo* glucose kinetics and pancreatic-insulin clamp procedure.** The infusion studies lasted a total of 360 min (**Fig. 3a**). At 0 min, a primed-continuous ICV infusion of either CPT1 inhibitors or control solution was initiated and maintained for the remainder of the study. TDGA (a gift from M. Guzman) was dissolved in DMSO, diluted into artificial cerebrospinal fluid (Harvard Apparatus) and provided as an ICV infusion at a rate of 50 pmol/h. ST1326 and ST1340 were dissolved in artificial cerebrospinal fluid and infused at a rate of 50 pmol/h. Before the pancreatic-insulin clamp studies, rats receiving ICV injection of vector control 3 d before the clamp procedure were 'pair-fed' with the experimental group receiving CPT1L-Ribo. A primed-continuous infusion of [^{3}H]glucose (40 µCi bolus, 0.4 µCi/min; New England Nuclear) purified by high-performance liquid chromatography (HPLC) was started at 120 min and continued for the duration of the study[11,16,17]. Finally, a pancreatic-insulin clamp[11,16,17] was initiated at 240 min and lasted for 2 h. This procedure involved the infusion of somatostatin (3 µg/kg per min), insulin (1 mU/kg per min) and glucose (as needed to prevent hypoglycemia). Glucose kinetics were calculated as described before[11,16,17].

Statistical analyses and protocol review. All values are presented as mean ± s.e.m. Comparisons among groups were made using analysis of variance or unpaired Student's *t* test as appropriate. The study protocol was reviewed and approved by the Institutional Animal Care and Use Committee of the Albert Einstein College of Medicine.

ACKNOWLEDGMENTS

This work was supported by grants from the National Institutes of Health (to L.R.; DK48321 and DK45024) and from the Albert Einstein College of Medicine Diabetes Research & Training Center. S.O. was the recipient of a postdoctoral fellowship and a Junior Faculty Award from the American Diabetes Association.

COMPETING INTERESTS STATEMENT

The authors declare competing financial interests (see the *Nature Medicine* website for details).

Received 3 July 2002; accepted 16 April 2003
Published online 18 May 2003; doi:10.1038/nm873

1. Hill, J.O. & Peters, J.C. Environmental contributions to obesity epidemic. *Science* **280**, 1371–1374 (1998).
2. Kopelman, P.G. & Hitman, G.A. Diabetes. Exploding type II. *Lancet* **352** (suppl. 4), SIV5 (1998).
3. Woods, S.C., Lotter, E.C., McKay, D.L. & Porte, D., Jr. Chronic intracerebroventricular infusion of insulin reduces food intake and body weight of baboons. *Nature.* **282**, 503–505 (1979).
4. Bruning, J.C. *et al.* Role of brain insulin receptor in control of body weight and reproduction. *Science* **289**, 2122–2125 (2000).
5. Friedman, J.M. Obesity in the new millennium. *Nature* **404**, 632–634 (2000).
6. Air, E.L. *et al.* Small molecule insulin mimetics reduce food intake and body weight and prevent development of obesity. *Nat. Med.* **8**, 179–183 (2002).
7. Schwartz, M.W., Woods, S.C., Porte, D. Jr., Seeley, R.J. & Baskin, D.G. Central nervous system control of food intake. *Nature* **404**, 661–671 (2000).
8. Ahima, R.S. *et al.* Role of leptin in the neuroendocrine response to fasting. *Nature* **382**, 250–252 (1996).
9. Wang, J., Liu, R., Hawkins, M., Barzilai, N. & Rossetti, L. A nutrient-sensing pathway regulates leptin gene expression in muscle and fat. *Nature* **393**, 684–688 (1998).
10. Loftus, T.M. *et al.* Reduced food intake and body weight in mice treated with fatty acid synthase inhibitors. *Science* 288, 2379–2381 (2000).
11. Obici, S. *et al.* Central administration of oleic acid inhibits glucose production and food intake. *Diabetes* **51**, 271–275 (2002).
12. Makimura, H. *et al.* Cerulenin mimics effects of leptin on metabolic rate, food intake, and body weight independent of the melanocortin system, but unlike leptin, cerulenin fails to block neuroendocrine effects of fasting. *Diabetes* 50, 733–739 (2001).
13. Shimokawa, T., Kumar, M.V. & Lane, M.D. Effect of a fatty acid synthase inhibitor on food intake and expression of hypothalamic neuropeptides. *Proc. Natl. Acad. Sci. USA* **99**, 66–71 (2002).
14. McGarry, G.D., Mannaert, G.P. & Foster, D.W. A possible role for malonyl-CoA in the regulation of hepatic fatty acid oxidation and ketogenesis. *J. Clin. Invest.* **60**, 265–270 (1977).
15. Zammit, V.A. Regulation of ketone body metabolism. A cellular perspective. *Diabetes Rev.* **2**, 132–155 (1994).
16. Obici, S. *et al.* Central melanocortin receptors regulate insulin action. *J. Clin. Invest.* **108**, 1079–1085 (2001).
17. Liu, L. *et al.* Intracerebroventricular (ICV) leptin regulates hepatic but not peripheral glucose fluxes. *J. Biol. Chem.* **273**, 31160–31167 (1998).
18. Miller, J.C., Gnaedinger, J.M. & Rapaport, S.I. Utilization of plasma fatty acid in rat brain: distribution of [^{14}C]palmitate between oxidative and synthetic pathways. *J. Neurochem.* **49**, 1507–1514 (1987).
19. Goto M. & Spitzer J.J. Fatty acids profiles of various lipids in the cerebrospinal fluid. *Proc. Exp. Biol. Med.* **136**, 1294–1296 (1971).
20. Briscoe, C.P. *et al.* The orphan G protein-coupled receptor GPR40 is activated by medium and long chain fatty acids. *J. Biol. Chem.* **278**, 11303–11311 (2003).
21. Lunzer, M.A., Manning, J.A. & Ockner, R.K. Inhibition of rat liver acetyl coenzyme A carboxylase by long chain acyl coenzyme A and fatty acid. *J. Biol. Chem.* **252**, 5483–5487 (1977).
22. Brun, T., Assimacopoulos-Jeannet, F., Corkey, B.E. & Prentki, M. Long-chain fatty acids inhibit acetyl-CoA carboxylase gene expression in the pancreatic beta-cell line INS-1. *Diabetes* **46**, 393–400 (1997).
23. Blazquez, C., Sanchez, C., Daza, A., Galve-Roperh, I. & Guzman, M. The stimulation of ketogenesis by cannabinoids in cultured astrocytes defines carnitine palmitoyltransferase I as a new ceramide-activated enzyme. *J. Neurochem.* **72**, 1759–1768 (1999).
24. Di Marzo, V. *et al.* Leptin-regulated endocannabinoids are involved in maintaining food intake. *Nature* **410**, 822–825 (2001).
25. Esser, V., Britton, C.H., Weis, B.C., Foster, D.W. & McGarry, J.D. Cloning, sequencing, and expression of a cDNA encoding rat liver carnitine palmitoyltransferase I. Direct evidence that a single polypeptide is involved in inhibitor interaction and catalytic function. *J. Biol. Chem.* **268**, 5817–5822 (1993).
26. Birikh, K.R., Heaton, P.A. & Eckstein, F. The structure, function and application of the hammerhead ribozyme. *Eur. J. Biochem.* **245**, 1–16 (1997).
27. Boussif, O. *et al.* A versatile vector for gene and oligonucleotide transfer into cells in culture and *in vivo*: polyethylenimine. *Proc. Natl. Acad. Sci. USA* **92**, 7297–7301 (1995).
28. Goula, D. *et al.* Size, diffusibility and transfection performance of linear PEI/DNA complexes in the mouse central nervous system. *Gene Ther.* **5**, 712–717 (1998).
29. Palkovits M. Isolated removal of hypothalamic or other brain nuclei of the rat. *Brain Res.* **59**, 449–450 (1973).
30. Obici, S., Feng, Z., Karkanias, G., Baskin, D.G. & Rossetti, L. Decreasing hypothalamic insulin receptors causes hyperphagia and insulin resistance in rats. *Nat. Neurosci.* **5**, 566–572 (2002).
31. Paxinos, G. & Watson, C. *The Rat Brain in Stereotaxic Coordinates* 3rd edn. (Academic Press, 1997).
32. Arduini, A. *et al.* Evidence for the involvement of carnitine-dependent long-chain acyltransferases in neuronal triglyceride and phospholipid fatty acid turnover. *J. Neurochem.***62**, 1530–1538 (1994).
33. Woldegiorgis, G., Spennetta, T., Corkey, B.E., Williamson, J.R. & Shrago, E. Extraction of tissue long-chain acyl-CoA esters and measurement by reverse-phase high-performance liquid chromatography. *Anal. Biochem.* **150**, 8–12 (1985).